Journal of Applied Electrochemistry **34**: 623–629, 2004.

Corrosion behaviour of niobium in sodium hydroxide solutions

A. ROBIN
Departamento de Engenharia de Materiais/DEMAR, Faculdade de Engenharia Química de Lorena/FAENQUIL, Polo Urbo-Industrial, Gleba AI-6, 12600-000 Lorena, SP - Brazil (e-mail: alain@demar.faenquil.br)

Received 5 September 2003; accepted in revised form 10 December 2003

Key words: corrosion, impedance, niobate, niobium, sodium hydroxide

Abstract

The electrochemical behaviour of niobium was investigated in sodium hydroxide solutions at different temperatures, using open-circuit potential (OCP) measurements, potentiodynamic polarization and electrochemical impedance spectroscopy (EIS). OCP and polarization measurements show that Nb is spontaneously active in 10, 15 and 30 wt % NaOH at 25, 50 and 75 °C. The anodic polarization curves in all cases show a dissolution/passivation peak followed by a current plateau, corresponding to Nb_2O_5 formation. The spontaneous active corrosion of Nb leads to the formation of soluble niobates that precipitate to sodium niobates. The evaluation of the corrosion current densities obtained from Tafel extrapolation of polarization curves and the polarization resistance values determined from EIS measurements indicates that the corrosion rates of niobium increase with increasing NaOH concentration and temperature.

1. Introduction

Niobium (Nb), as well as the other valve metals, spontaneously forms a compact, nonporous and stable oxide film (Nb_2O_5) which provides good corrosion resistance to the base metal in a wide variety of media, specially acid and neutral solutions [1]. The thickness of this oxide film grows spontaneously and slowly in oxidizing solutions, but rapidly under controlled anodic polarization. Most work on Nb behaviour in aqueous media deals with the study of the corrodability, electrical properties and chemical characterization of this anodic oxide film in neutral, acid and alkaline solutions [2–14]. Little work is available on the spontaneous behaviour of Nb in alkaline solutions using electrochemical methods. It was shown that the naturally air-formed oxide film on Nb is stable or subject to slow dissolution in low alkali concentration at low temperature [2, 3, 5, 11], but electrochemical data in concentrated solutions at high temperatures are limited [14, 15].

The purpose of this work is to study the electrochemical behaviour of commercially pure Nb in sodium hydroxide (NaOH) solutions at different concentrations and temperatures. This investigation is based on open-circuit, potentiodynamic and electrochemical impedance measurements.

2. Experimental details

Cylindrical test specimens (8 mm dia. × 15 mm length) were machined from commercially pure Nb ingot, obtained by double melting in electron beam furnace (ES-2/18/300, Leybold-Heraeus), and mounted in PTFE holders. The chemical composition of Nb is as follows: O < 50, N < 30, C < 30, Ta = 2000, Al < 10, Si < 30, Fe < 10 (ppm by weight).

The cross-sectional area of the electrodes (0.5 cm^2) was mechanically ground with emery paper up to 600 grit, degreased with acetone, rinsed with distilled water and dried with air.

The solutions, prepared from analytical reagents and deionized water, were 10, 15 and 30 wt % NaOH. The solutions were naturally aerated and no stirring was operated during the experiments. The temperature of the solutions was maintained at 25, 50 and 75 ± 2 °C. The counter electrode was a square-shaped platinum sheet of 18 cm^2 area. All potentials were referred to the saturated calomel electrode (SCE) potential (= +0.242 V vs SHE).

E/t and polarization measurements were performed using a PAR 273A potentiostat controlled with a microcomputer through M352 corrosion software. Electrochemical impedance spectroscopy (EIS) measurements were carried out at open-circuit potentials using an electrochemical interface (Solartron model 1287A) and a frequency response analyser (Solartron model 1260 A), controlled by a microcomputer through Ecorr/Zplot (Solartron model 125587S) software.

Prior to cathodic and anodic polarization, the working electrodes were immersed in the solutions until stabilization of the open-circuit potential, taking the immersion moment as zero time. The polarization studies were carried out potentiodynamically with

1 mV s^{-1} potential sweep rate. After each polarization experiment, the samples were reground with emery papers to a 600-grit finish in order to remove any product formed on the metal surface which could affect the following tests, rinsed with distilled water, dried and transferred quickly in the NaOH solution. The impedance measurements were made at open-circuit potential using a sinusoidal signal of 10 mV amplitude and frequencies in the 0.1 Hz–100 kHz range.

Some immersion tests were performed and the Nb coupons were observed by scanning electron microscopy (Leo VP-1450 SEM) and analysed using X-ray diffractometry (Siefert XRD).

3. Results and discussion

3.1. *Open-circuit potential measurements*

Figure 1 presents the evolution of the open-circuit potential (OCP) of Nb as a function of exposure time in 10% NaOH at all temperatures and at 50 °C in all NaOH solutions. The E/t curves have the same shape. The OCP drops in the negative direction and stabilizes for long exposure times. The decrease in OCP with time is indicative of the dissolution of the protective air-formed oxide and the subsequent surface activation. This behaviour was observed for all the other temperatures and NaOH concentrations under study.

Figure 2 shows the variation of the corrosion potential (OCP value measured for the longest exposure times) as a function of NaOH concentration and temperature. The corrosion potential shifts in the negative direction as the NaOH concentration and temperature increase, which is indicative of a higher aggressiveness of the solution. These results are in accordance with published data for Nb in concentrated NaOH solutions at 30 °C [3, 5].

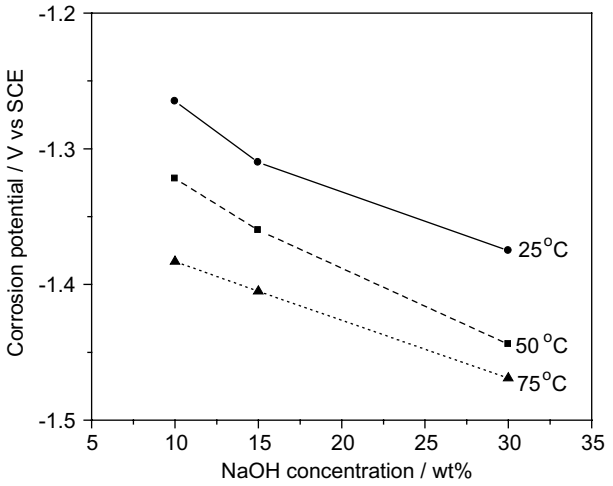

Fig. 2. Variation of Nb corrosion potential as a function of NaOH concentration and temperature.

The steady state potentials are in the range from −1.469 to −1.265 V vs SCE and are close to the values reported for abraded and anodized Nb measured after 3 h immersion in 3 to 5 N (11 to 17 wt %) NaOH at 30 °C, nearly −1.2 V vs SCE [3, 5].

3.2. *Polarization results*

Figures 3 to 5 show the polarization curves of Nb obtained for all temperatures, in 10, 15 and 30% NaOH, respectively. The shape of the curves is very similar, suggesting that the reactions at the metal–solution interface are the same. Nevertheless, an increase of current densities is observed as temperature and NaOH concentration increase.

The cathodic curves present a characteristic Tafel behaviour and the cathodic current density shifts to higher value as temperature and NaOH concentration increase (Figures 3 to 5).

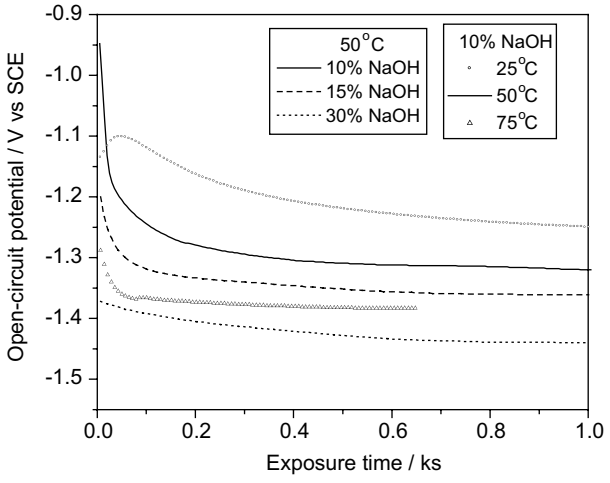

Fig. 1. Variation of Nb open-circuit potential in 10% NaOH solutions at 25, 50 and 75 °C, and in 10, 15 and 30% NaOH at 50 °C as a function of exposure time.

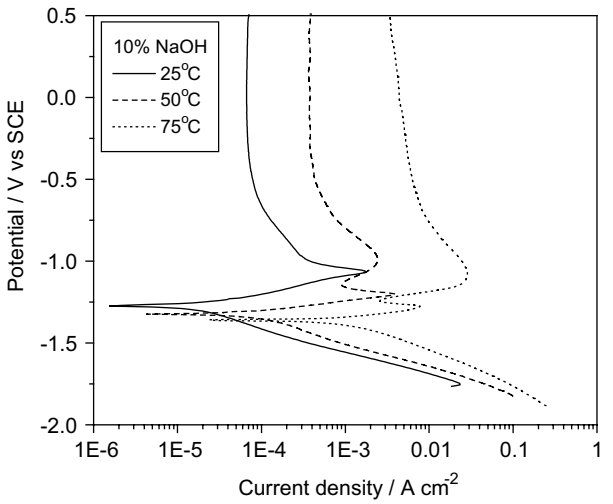

Fig. 3. Anodic and cathodic polarization curves of Nb in 10 wt % NaOH solutions.

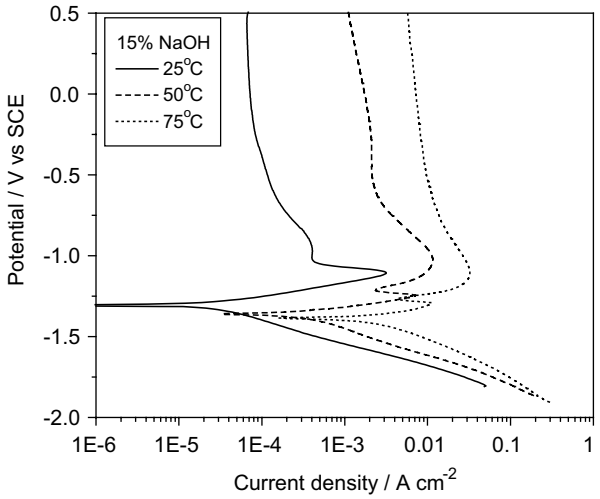

Fig. 4. Anodic and cathodic polarization curves of Nb in 15 wt % NaOH solutions.

The main cathodic reactions in aqueous solutions at high pH are the reduction of dissolved oxygen and direct reduction of water, the latter causing hydrogen evolution. At pH close to 14, the equilibrium potentials for the H_2O/O_2 and H_2/H_2O systems are +0.404 V vs SHE (or +0.162 V vs SCE) and −0.826 V vs SHE (or −1.068 V vs SCE), respectively [16]. Considering that the OCP values for Nb in 10, 15 and 30 wt % NaOH at 25 °C to 75 °C are in the range from −1.469 to −1.265 V vs SCE (Figure 2), the cathodic reaction that dominates on metallic Nb under these conditions is

$$2\,H_2O + 2\,e^- \rightarrow H_2 + 2\,OH^- \qquad (1)$$

The evolution of gaseous products observed during cathodic polarization corroborates the occurrence of this reaction.

The cathodic Tafel slopes, as expected, increase with increasing temperature but do not depend significantly on NaOH concentration (Table 1). The values obtained

Table 1. Cathodic Tafel slope (V decade^{-1}) for H_2 evolution on Nb in NaOH solutions

NaOH concentration /wt %	Temperature /°C		
	25	50	75
10	−0.136	−0.152	−0.207
15	−0.136	−0.163	−0.206
30	−0.159	−0.170	−0.201

in 10 and 15 wt % NaOH at 25 °C are close to the value of Rotinyan et al. [17] in 1 M (4 wt %) NaOH at the same temperature, −0.140 V decade^{-1}.

The anodic curves (Figures 3 to 5) present a dissolution/passivation peak split in two components (a sharp peak (1st) at −1.2 V, followed by a broad one (2nd) at −1.0 V vs SCE), and a current plateau at more noble potential ($E > -0.5$ V vs SCE). The second peak is not well defined at room temperature. Baruffaldi et al. [14] obtained anodic polarization curves of similar shape for Nb in 5 M NaOH at 50 °C.

The active/passive transition on the anodic curves confirms the spontaneous active behaviour of Nb in these temperature/NaOH concentration conditions, pointed out from the OCP measurements.

The current density of both peaks (measured at the maximum value) increases as temperature and NaOH concentration increase (Figure 6). Nevertheless, the current density of the second peak shows a more pronounced increase and presents higher values than the first peak at 50 and 75 °C in 15 and 30% NaOH. The potential of the first peak shifts in the negative direction as temperature and NaOH concentration increase, whereas the potential of the second peak does not vary significantly.

The current density in the plateau region also increases as temperature and NaOH concentration increase (Figures 3 to 5).

Anodic voltammetric experiments carried out from OCP in 15 wt % NaOH at 50 °C using 1 to 100 mV s^{-1}

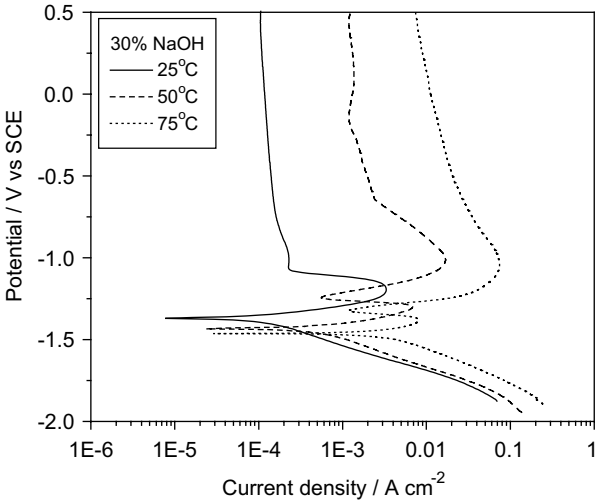

Fig. 5. Anodic and cathodic polarization curves of Nb in 30 wt % NaOH solutions.

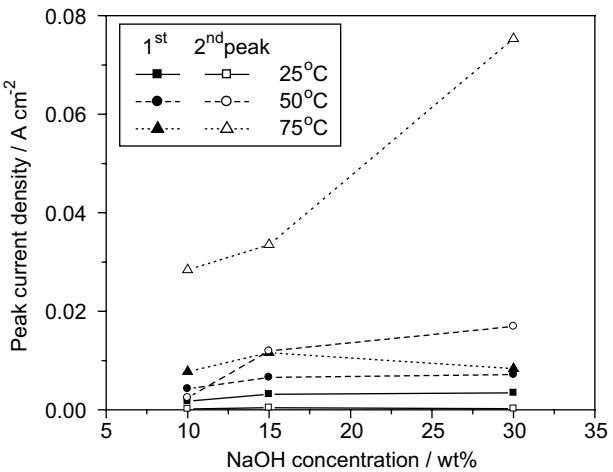

Fig. 6. Peak current densities as a function of NaOH concentration and temperature.

potential scan rates (Figure 7(a)) show that the current density of the first peak increases linearly with the square root of all applied scan rates, whereas this behaviour is only observed up to 30 mV s^{-1} for the second peak (Figure 7(b)). Above 30 mV s^{-1}, the increase of the current density of the second peak is not significant.

The observed dependence of peak current densities on NaOH concentration and potential scan rate is indicative that the hydroxyl ions take part in the corresponding reactions and that these reactions are diffusion controlled.

Niobium samples were polarized in 15 wt % NaOH solutions at 50 °C for 120 min at −1.22 (first current peak), −1.16, −1.0 (second current peak) and −0.5 V vs SCE (current plateau) and analysed by SEM and XRD. The corresponding i/t curves show that the current density decreases with exposure time (Figure 8). For −1.22 and −0.5 V vs SCE applied potentials, the dissolution current density decreases rapidly to low values and an adherent film is formed. For −1.16 and −1.0 V vs SCE, a not adherent layer is produced and the current values are higher. Both products are constituted of needle-like crystallites (Figure 9(a) and (b)) and presented the same XRD spectrum (Figure 10). The spectrum was indexed using the JCPDS diffraction data of $Na_8Nb_6O_{19}$–13 H_2O and $Na_{14}Ta_{12}O_{37}$–31 H_2O [18].

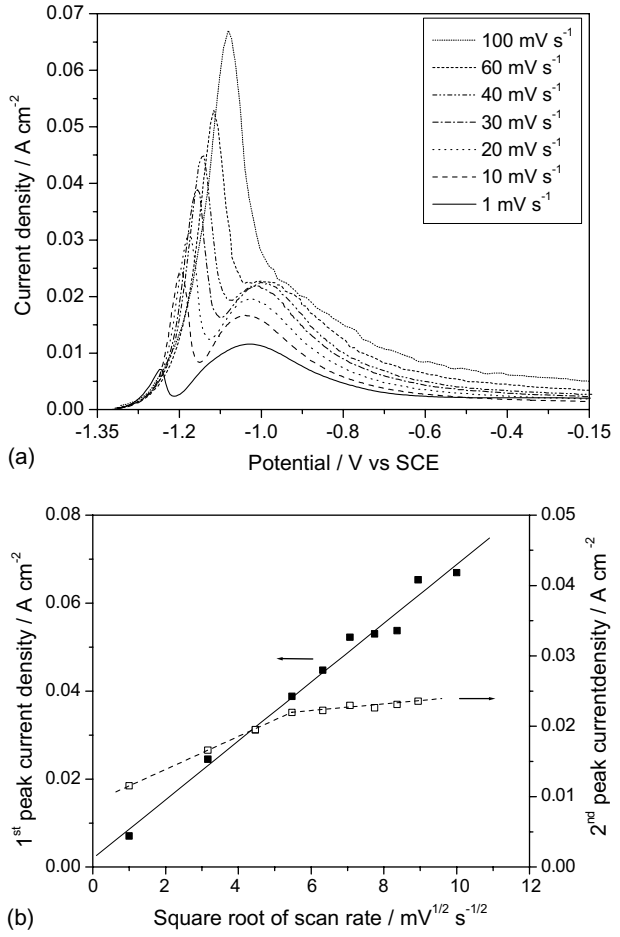

Fig. 7. (a) Anodic voltammograms of Nb in 15 wt % NaOH at 50 °C for different potential scan rates; (b) peak current densities as a function of the square root of scan rate.

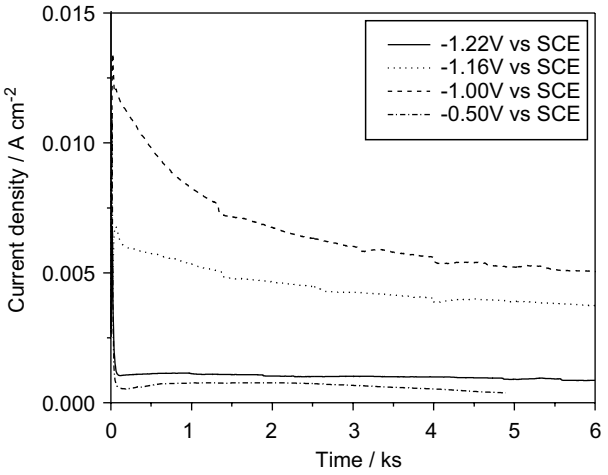

Fig. 8. Current density as a function of exposure time at −1.22, −1.16, −1.0 and −0.5 V vs SCE applied potentials in 15 wt % NaOH solutions at 50 °C.

The XRD spectrum of $Na_{14}Nb_{12}O_{37}$–31 H_2O was not available in the diffraction databases but it may be expected that its XRD pattern is similar to that of $Na_{14}Ta_{12}O_{37}$–31 H_2O, due to same ionic radius of Nb(V) and Ta(V). The good concordance between the spectra of the films and both compounds attests that $Na_8Nb_6O_{19}$–13 H_2O and $Na_{14}Nb_{12}O_{37}$–31 H_2O form during prolonged polarization in both active and passive regions. The same corrosion products were also detected after long exposure time of Nb at OCP.

At OCP and in the peak region, Nb dissolves under the effect of the hydroxyl ions with formation of soluble niobates, which precipitate when their solubility limit is reached. The increase of solubility with increasing temperature explains the corresponding increase in peak current densities.

At higher potentials (plateau region), passivation occurs due to the formation of Nb_2O_5 oxide. In this potential range, the mechanism involves simultaneously the anodic film formation and its chemical dissolution to niobate ions.

It can be assumed that the formation of sodium niobium oxide hydrates (e.g., $Na_8Nb_6O_{19}$) occurs by a dissolution–precipitation mechanism, according to the following:

At OCP and in the peak region

$$6\,Nb + 38\,OH^- \rightarrow Nb_6O_{19}^{8-} + 19\,H_2O + 30\,e^- \quad \text{(electrochemical dissolution)} \tag{2}$$

$$Nb_6O_{19}^{8-} + 8\,Na^+ \rightarrow Na_8Nb_6O_{19} \quad \text{(precipitation)} \tag{3}$$

In the passive region

$$2\,Nb + 10\,OH^- \rightarrow Nb_2O_5 + 5\,H_2O + 10\,e^- \quad \text{(anodic film formation)} \tag{4}$$

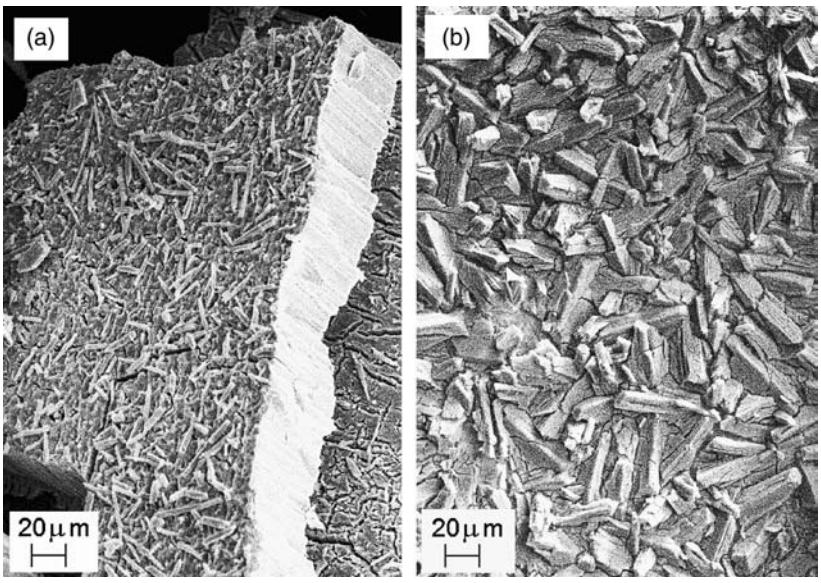

Fig. 9. SEM photographs of corrosion products after polarization of Nb in 15 wt % NaOH at 50 °C for 120 min (a) at −1.16 V vs SCE and (b) at −0.5 V vs SCE.

$$3\,Nb_2O_5 + 8\,OH^- \rightarrow Nb_6O_{19}^{8-} + 4\,H_2O \quad \text{(chemical dissolution)} \tag{5}$$

$$Nb_6O_{19}^{8-} + 8\,Na^+ \rightarrow Na_8Nb_6O_{19} \quad \text{(precipitation)} \tag{6}$$

These mechanisms are also corroborated by the results of Baruffaldi et al. [15], who detected by XPS analyses the presence of Na niobate after prolonged polarization of Nb at peak potential in 3 M NaOH at 60 °C, and Na niobate + Nb_2O_5 oxide after polarization in plateau region.

The corrosion current densities of Nb, determined from the polarization curves using the extrapolation method, increase with the increase of both NaOH concentration and temperature (Figure 11). The variation of ln (corrosion current density) with the reciprocal temperature, T^{-1}, is nearly linear, which depicts the thermally activated character of the processes occurring at the Nb surface in NaOH solutions. The activation energy obtained from the slope of the linear fitted curves, using Arrhenius' law, is 75 ± 6 kJ mol^{-1}.

3.3. *Electrochemical impedance measurements*

EIS experiments were also carried out at OCP for the different NaOH concentrations and temperatures (Figure 12). The Nyquist diagrams present depressed semicircles and the Bode diagrams show a linear relation (slope in the range from −0.82 to −0.9) between log |Impedance| and log (Frequency). The phase angle is in the range from −62° to −76° for the intermediate

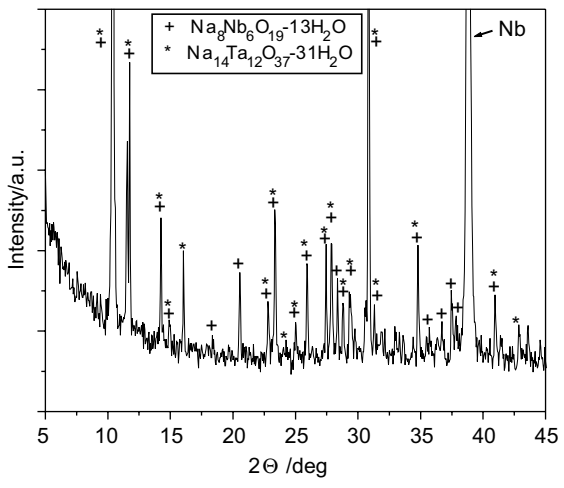

Fig. 10. XRD pattern of corrosion products after polarization of Nb at −0.5 V vs SCE in 15 wt % NaOH at 50 °C for 120 min.

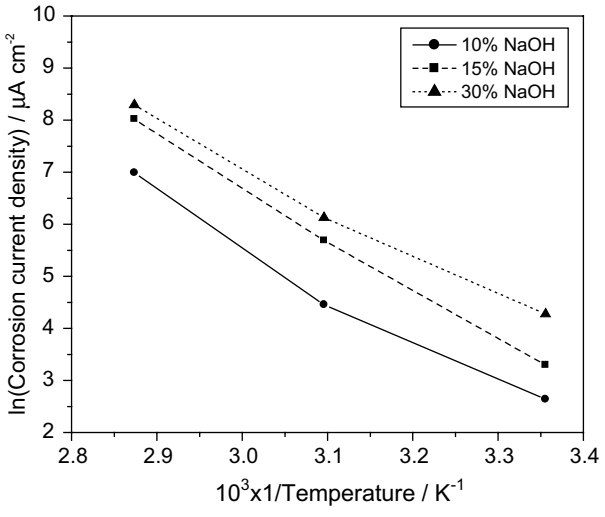

Fig. 11. Variation of Nb corrosion current density as a function of NaOH concentration and temperature.

frequencies. This is characteristic of a predominantly capacitive behaviour.

Badawy et al. [10, 19, 20] obtained good results representing the electrode–electrolyte interface for Ta in aqueous solutions by the simple Randles equivalent circuit. This circuit consists of a capacitor parallel to a resistor and the solution resistance is simulated by a series resistor. In our case, the interface is better described by a circuit consisting of a constant-phase element (CPE) with a parallel resistor R_P, and a series resistor R_S to represent the electrolyte resistance (Figure 13). Such a model was shown to be suitable for this type of study [11, 21–23]. The impedance of the CPE is defined as

$$Z_{CPE} = \frac{1}{(i\omega)^n C} \tag{7}$$

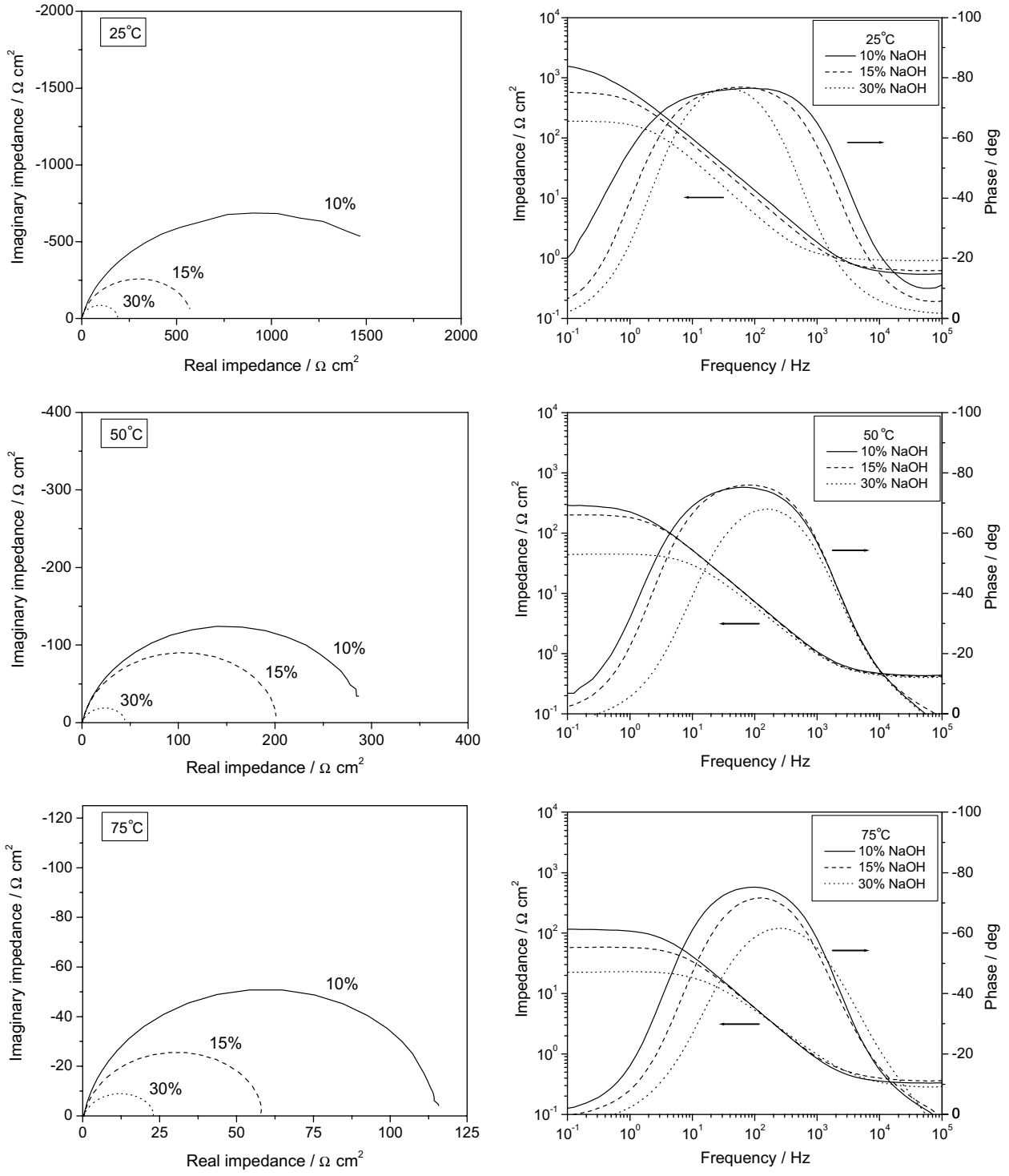

Fig. 12. Nyquist and Bode diagrams for Nb at OCP as a function of NaOH concentration and temperature.

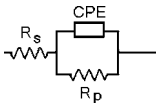

Fig. 13. Equivalent circuit model used for fitting of experimental EIS data. (CPE: constant-phase element; R_P: polarization resistance; R_S: electrolyte resistance).

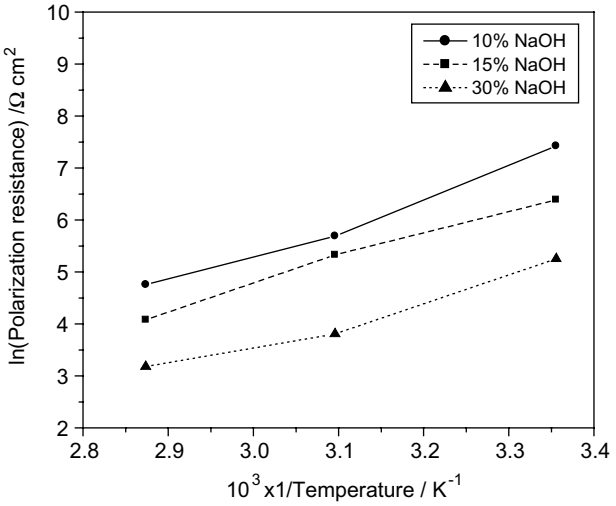

Fig. 14. Polarization resistance of Nb at OCP as a function of NaOH concentration and temperature.

with the value of n being related to a nonuniform current distribution due to surface roughness or non-homogeneity. This model was shown to fit our experimental data better than the R–C model. The CPE parameter n and the phase angle for intermediate frequencies deduced from the impedance data for all NaOH concentrations and temperatures, are in the 0.82/0.90 and −62°/−76° ranges, which indicates that the interface does not behave as an ideal capacitor ($n = 1$ and phase angle −90°), in agreement with the need of using CPE as a model for the system.

The diameter of the semicircles decreases with increase in both temperature and NaOH concentration (Figure 12), which indicates a decrease in corrosion resistance. The polarization resistance extrapolated from the fitted curves in the Nyquist diagrams to the Z values corresponding to the lowest frequency is shown in Figure 14. The decrease of polarization resistance with increasing of temperature and NaOH concentration depicts the decrease in corrosion resistance, according to the results obtained from corrosion current densities.

4. Conclusions

Nb undergoes self-activation in 10, 15 and 30 wt % NaOH at 25, 50 and 75 °C, due to the spontaneous dissolution of its superficial air-formed oxide and remains in the active state. Nb forms soluble niobates that precipitate as sodium niobates, as identified by SEM observation and XRD analysis.

The anodic polarization curves are characterized by a dissolution/passivation current peak followed a passive current plateau.

Prolonged polarization in the passive potential range also leads to the formation of sodium niobates.

The spontaneous corrosion current density, critical current density and passive current density increase with increase in NaOH concentration and temperature, which is indicative of a decrease in corrosion resistance.

References

1. T.L. Yau and R.T. Webster, *in* 'Corrosion', ASM Handbook, Vol. 13 (ASM International, Metals Park, OH, 1993), p. 722.
2. T. Hurlen, H. Bentzen and S. Hornkjol, *Electrochim. Acta* **32** (1987) 1613.
3. W.A. Badawy, A.G. Gad-Allah and H.H. Rehan, *J. Appl. Electrochem.* **17** (1987) 559
4. F. Di Quarto, S. Piazza and C. Sunseri, *Electrochim. Acta* **35** (1990) 99.
5. A.G. Gad-Allah, *J. Appl. Electrochem.* **21** (1991) 346.
6. S. Hornkjol, *Electrochem. Acta* **36** (1991) 1443.
7. C.V. D'Alkaine, L.M.M. de Souza and F.C. Nart, *Corros. Sci.* **34** (1993) 109.
8. C.V. D'Alkaine, L.M.M. de Souza and F.C. Nart, *Corros. Sci.* **34** (1993) 117.
9. C.V. D'Alkaine, L.M.M. de Souza and F.C. Nart, *Corros. Sci.* **34** (1993) 129.
10. F.M. Al-Kharafi and W.A. Badawy, *Electrochim. Acta* **40** (1995) 2623.
11. G.E. Cavigliasso, M.J. Esplandiu and V.A. Macagno, *J. Appl. Electrochem.* **28** (1998) 1213.
12. A.D. Modestov and A.D. Davydov, *J. Electroanal. Chem.* **460** (1999) 214.
13. B-X. Huang, K. Wang, J.S. Church and Y-S. Li, *Electrochim. Acta* **44** (1999) 2571.
14. C. Baruffaldi, U. Casellato, S. Cattarin, M. Musiani, B. Tribollet and B. Vercelli, *Electrochim. Acta* **47** (2002) 2989.
15. C. Baruffaldi, R. Bartoncello, S. Cattarin, P. Guerriero and M. Musiani, *J. Electroanal. Chem.* **545** (2003) 65.
16. M. Pourbaix, Atlas of Electrochemical Equilibria in Aqueous Solutions (Pergamon Press, New York, 1966).
17. A.L. Rotinyan and N.M. Koshevnikova, *Zh. Fiz. Khim.* **37** (1963) 1818.
18. 'Powder Diffraction Files – Inorganic Phases', JCPDS International Centre for Diffraction Data (Swarthmore, Pa, USA, 1988).
19. W.A. Badawy, S.S. Elegamy and Kh.M. Ismail, *British. Corr. J.* **28** (1993) 133.
20. W.A. Badawy and Kh.M. Ismail, *Electrochim. Acta* **38** (1993) 2231.
21. A. Robin, *J. Appl. Electrochem.* **33** (2003) 37.
22. J.R. MacDonald, *J. Electroanal. Chem.* **233** (1987) 25.
23. M.J. Esplandiu, E.M. Patrito and V.A. Macagno, *Electrochim. Acta* **40** (1995) 809.